Cell Reports

Article

Targeting Bim via a lncRNA *Morrbid* Regulates the Survival of Preleukemic and Leukemic Cells

Graphical Abstract

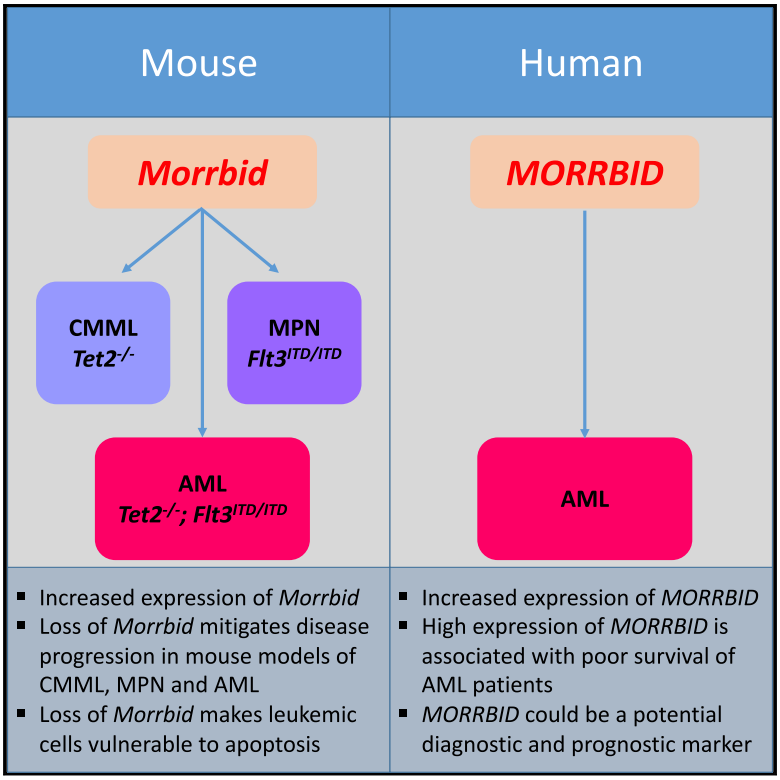

Highlights

- Hyperactivation of *Morrbid* and reduced apoptosis in *Tet2*$^{-/-}$*;Flt3* $^{ITD/ITD}$ AML
- *Morrbid* modulates Tet2$^{-/-}$ CMML, Flt3$^{ITD/ITD}$ MPN, and Tet2$^{-/-}$;Flt3$^{ITD/ITD}$ AML
- Genetic loss of *Morrbid* makes leukemic cells vulnerable to apoptosis
- Increased expression of *MORRBID* in human AML correlates with poor survival

Authors

Zhigang Cai, Fabiola Aguilera, Baskar Ramdas, ..., Chi Zhang, Jorge Henao-Mejia, Reuben Kapur

Correspondence

zcai@iupui.edu (Z.C.), rkapur@iupui.edu (R.K.)

In Brief

Cai et al. report that *MORRBID*/*Morrbid* expression is aberrantly increased in human AML patients and mouse models for CMML, MPN, and AML. Genetic loss of *Morrbid* makes leukemic cells vulnerable to apoptosis and mitigates the progression of myeloid neoplasms. High expression of *MORRBID* in humans is associated with poor survival of AML patients.

Cai et al., 2020, Cell Reports *31*, 107816
June 23, 2020
https://doi.org/10.1016/j.celrep.2020.107816

CellPress

Cell Reports

CellPress
OPEN ACCESS

Article

Targeting Bim via a lncRNA *Morrbid* Regulates the Survival of Preleukemic and Leukemic Cells

Zhigang Cai,[1,2,*] Fabiola Aguilera,[1] Baskar Ramdas,[1] Swapna Vidhur Daulatabad,[3] Rajneesh Srivastava,[3] Jonathan J. Kotzin,[4] Martin Carroll,[4] Gerald Wertheim,[4] Adam Williams,[5] Sarath Chandra Janga,[3] Chi Zhang,[6] Jorge Henao-Mejia,[4,7,8] and Reuben Kapur[1,2,9,*]

[1]Herman B Wells Center for Pediatric Research, Indiana University School of Medicine, Indianapolis, IN, USA
[2]Department of Microbiology and Immunology, Indiana University School of Medicine, Indianapolis, IN, USA
[3]School of Informatics and Computing, Indiana University–Purdue University Indianapolis, Indianapolis, IN, USA
[4]Department of Pathology and Laboratory Medicine, University of Pennsylvania, Philadelphia, PA, USA
[5]The Jackson Laboratory for Genomic Medicine, Farmington, CT, USA
[6]Department of Medical and Molecular Genetics, Indiana University School of Medicine, Indianapolis, IN, USA
[7]Institute for Immunology, Perelman School of Medicine, University of Pennsylvania, Philadelphia, PA, USA
[8]Division of Protective Immunity, Children's Hospital of Philadelphia, Philadelphia, PA, USA
[9]Lead Contact
*Correspondence: zcai@iupui.edu (Z.C.), rkapur@iupui.edu (R.K.)
https://doi.org/10.1016/j.celrep.2020.107816

SUMMARY

Inhibition of anti-apoptotic proteins BCL-2 and MCL-1 to release pro-apoptotic protein BIM and reactivate cell death could potentially be an efficient strategy for the treatment of leukemia. Here, we show that a lncRNA, *MORRBID*, a selective transcriptional repressor of *BIM*, is overexpressed in human acute myeloid leukemia (AML), which is associated with poor overall survival. In both human and animal models, *MORRBID* hyperactivation correlates with two recurrent AML drivers, *TET2* and *FLT3*^{ITD}. Mice with individual mutations of *Tet2* or *Flt3*^{ITD} develop features of chronic myelomonocytic leukemia (CMML) and myeloproliferative neoplasm (MPN), respectively, and combined presence results in AML. We observe increased levels of *Morrbid* in murine models of CMML, MPN, and AML. Functionally, loss of *Morrbid* in these models induces increased expression of Bim and cell death in immature and mature myeloid cells, which results in reduced infiltration of leukemic cells in tissues and prolongs the survival of AML mice.

INTRODUCTION

One of the well-recognized hallmarks of cancer, including acute myeloid leukemia (AML), is its capability to evade cell death, which may also act as an underlying mechanism of drug resistance and/or tumor relapse in certain cancer therapies (Hanahan and Weinberg, 2011; McBride et al., 2019; Merino et al., 2018). It has been almost 30 years since the identification of BCL-2 and its family members in regulating cell apoptosis (anti-apoptosis: BCL-2, BCL-lnctnXL, and MCL-1; pro-apoptosis: BIM, BID, BAX, and BAK). The anti-apoptosis proteins of the BCL-2 family execute their function by sequestering pro-apoptosis proteins and preventing the creation of pores in the mitochondrial outer membrane via protein-protein interactions (Ashkenazi et al., 2017; Huang et al., 2019; Yang et al., 2019). Repressing the expression of anti-apoptosis protein via gene silencing or inhibiting such protein-protein interaction via BH3 mimetics are therefore emerging as novel targeting treatments for cancer, including several hematological malignancies in which BCL-2 and/or MCL-1 are aberrantly activated in leukemic stem cells (LSCs) or leukemic blasts. Indeed, venetoclax (ABT-199), an oral BCL-2 inhibitor, has been approved for the treatment of chronic lymphocytic leukemia and elderly patients with AML (DiNardo et al., 2019). Similarly, inhibition of MCL-1 via S64315 or AMG-176 as a single-agent therapy or in combination with BCL-2 inhibitor and other drugs is in clinical trials for AML treatment (Anstee et al., 2019; Caenepeel et al., 2018; Ramsey et al., 2018; Teh et al., 2018). Although BCL-2 itself is an important player in tumorigenesis and represents an important therapeutic target, *in vivo* stimulation of the expression of pro-apoptosis proteins in AML treatment (e.g., BIM) has not been studied in preclinical models (Shukla et al., 2017).

AML is a genetically and cellularly heterogenous clonal blood cancer caused by driver mutations that are able to transform hematopoietic stem cells (HSCs) to LSCs. The most prevailing ones include acute myelomonocytic leukemia (French-American-British [FAB] classification, M4) and acute monocytic leukemia (M5), where both mature myeloid cells and progenitors are leukemic and redundant. The recurrent mutations in M4 and M5 AML include genes encoding components of the signaling pathway and epigenetic regulations, such as the gain-of-function mutation *FLT3*$^{ITD/+}$ and the loss-of-function mutation *TET2*$^{+/-}$. Indeed, using murine models, recent studies suggest that mutations in *Tet2* define a preleukemic condition in HSCs and may induce clonal hematopoiesis of indeterminate potential (CHIP), which is a strong risk factor for blood cancer (Jaiswal and Ebert,

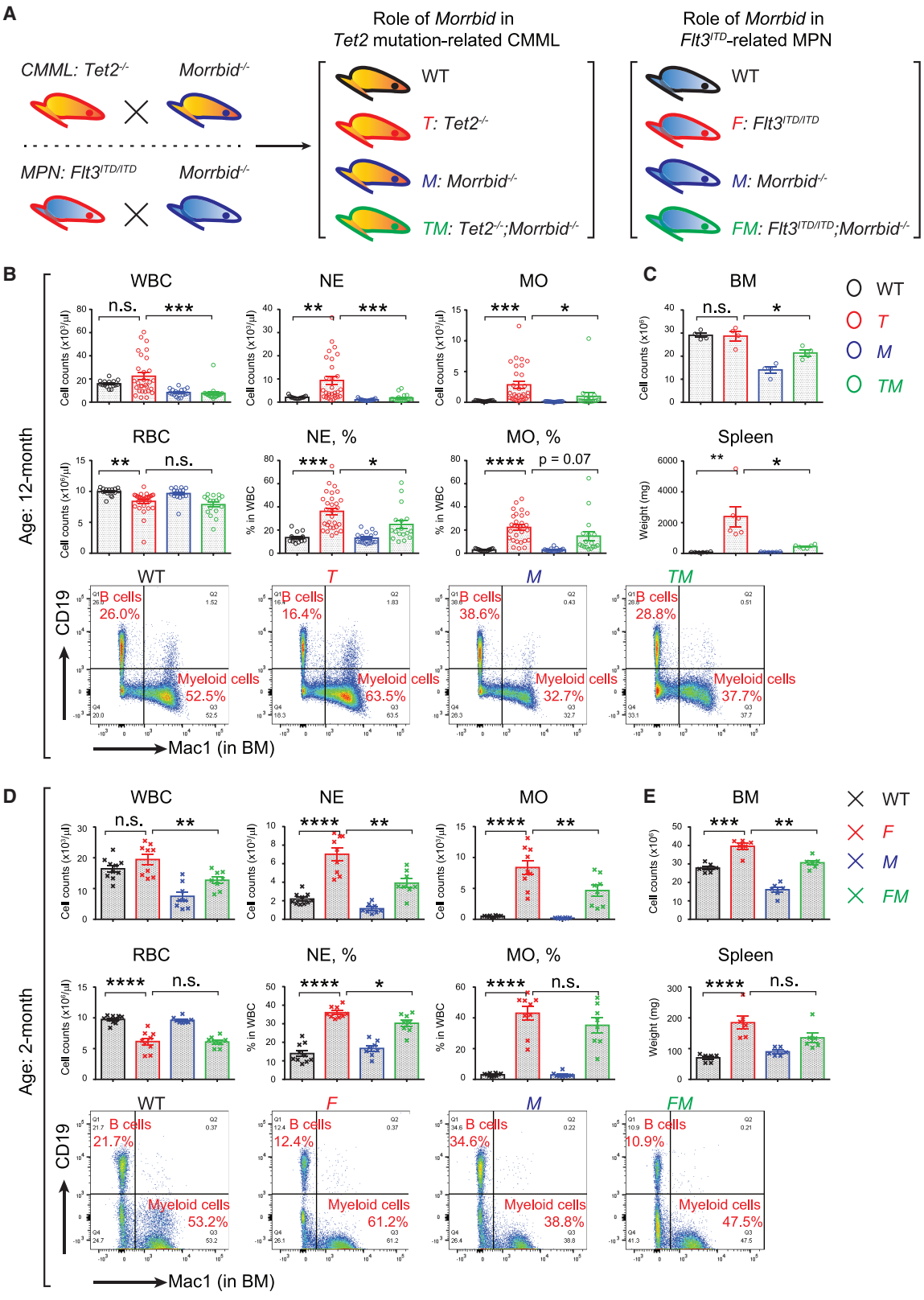

(legend on next page)

2019). Acquisition of additional mutations such as *Flt3*$^{ITD/+}$ in pre-leukemic cells bearing loss of *Tet2* results in the development of full-blown AML (Shih et al., 2015). Furthermore, the *Tet2*$^{-/-}$; *Flt3*$^{ITD/ITD}$ model of AML, the preleukemic model bearing *Tet2* loss, and a murine model expressing a knockin allele of *Flt3*^{ITD} manifest several cardinal features of human AML, chronic myelomonocytic leukemia (CMML), and myeloproliferative neoplasm (MPN), respectively (Chu et al., 2012; Moran-Crusio et al., 2011; Shih et al., 2015). Use of these clinically relevant models of myeloid neoplasm allow for validation of targets that are likely to provide best insight into human leukemia and its genetic drivers.

We have recently shown that the evolutionarily conserved novel long non-coding RNA (lncRNA) *Morrbid* is specifically expressed in myeloid cells and uniquely represses the expression of the pro-apoptotic gene *Bim* via DNA loop in *cis* to regulate the lifespan of myeloid cells (Kotzin et al., 2016). *Morrbid*$^{-/-}$ mice manifest inefficient production of innate immune cells (~50% of wild-type [WT] levels) but have normal activity and lifespan (Kotzin et al., 2016). Since *Morrbid* is specifically expressed in myeloid cells (i.e., neutrophils [NEs], monocytes [MOs], and eosinophils), but not in other cell types under physiologic conditions, the uniqueness of its expression pattern and function offers a great advantage and opportunity to test if it is required for the onset and progression of myeloid-related diseases, including various myeloid neoplasms. In the present study, we have characterized the role of lncRNA *MORRBID*/*Morrbid* and its target, BIM, in regulating the survival of preleukemic and leukemic cells.

RESULTS AND DISCUSSION

Role of *Morrbid* in Murine Models of CMML and MPN

Our recent study has defined the role of *Morrbid* in inflammation and *Tet2*-mutation induced aberrant emergency granulopoiesis and clonal hematopoiesis (Cai et al., 2018). We here first compared the role of *Morrbid* in driving *Tet2*-mutation-induced CMML and *Flt3*^{ITD}-mutation-induced MPN over an adequate lifetime, since CMML is a chronic disease in the elderly population (Figure 1A; Chu et al., 2012; Lee et al., 2007; Mead et al., 2013; Mead et al., 2017; Moran-Crusio et al., 2011). We generated *Tet2*$^{-/-}$; *Morrbid*$^{-/-}$ double homozygous mice along with all the controls. A large cohort of these mice was allowed to age and subsequently analyzed for peripheral blood (PB) changes. Consistent with previous studies, as seen in Figure 1B, although the average count of white blood cells (WBCs) in aged *Tet2*$^{-/-}$ mice is higher than that in WT controls, the counts of WBCs in each *Tet2*$^{-/-}$ individual mouse are highly variable relative to controls, suggesting that the onset and penetration of the CMML-like disease in each individual is different in the large cohort. However, the increase in average value of WBC counts observed in *Tet2* deficient mice was normalized and not highly variable in *Tet2*$^{-/-}$; *Morrbid*$^{-/-}$ mice (Figure 1B). Importantly, a similar and significant reversal in the increase in absolute number of NEs and MOs was observed in *Tet2*$^{-/-}$; *Morrbid*$^{-/-}$ mice compared to *Tet2*$^{-/-}$ mice. Likewise, the increase in the frequency of NEs and MOs observed in *Tet2*$^{-/-}$ mice was also rescued in the absence of *Morrbid*, along with the decrease in bone marrow (BM) cellularity and spleen weight (Figure 1B). Overall, while the percentages of NEs and MOs in *Tet2*$^{-/-}$; *Morrbid*$^{-/-}$ mice remained higher than WT controls, they were significantly lower than that observed in *Tet2*$^{-/-}$ mice (Figure 1B). In contrast, no improvement in red blood cell (RBC) counts was observed in *Tet2*$^{-/-}$; *Morrbid*$^{-/-}$ mice, suggesting that *Morrbid* does not impact the reduction in RBCs observed in aged *Tet2*$^{-/-}$ mice (Figure 1B).

Compared to *Flt3*$^{ITD/+}$ mice, *Flt3*$^{ITD/ITD}$ mice develop an early onset and full penetration of MPN-like phenotype via activation of STAT signaling, which eventually results in the activation of anti-apoptotic proteins BCL-2 or MCL-1 (Chu et al., 2012; Kikushige et al., 2008; Mead et al., 2013, 2017; Naganna et al., 2019). These mice develop several cardinal features of human MPN-like disease, including enhanced NE and MO counts, splenomegaly, and hyperceullular BM (Figures 1D and 1E). To determine the extent to which these changes are regulated by *Morrbid*-induced Bim repression, we generated mice lacking *Morrbid* and expressing *Flt3*$^{ITD/ITD}$ (*Flt3*$^{ITD/ITD}$; *Morrbid*$^{-/-}$). Similar to the results seen in the Tet2-deficiency-driven CMML model lacking *Morrbid*, we observed that loss of *Morrbid* in the setting of *Flt3*$^{ITD/ITD}$ expression rescued the abnormal phenotypes observed in *Flt3*$^{ITD/ITD}$, including high NE and MO counts in PB (Figure 1D). Interestingly, while RBC and spleen size were not significantly corrected in the *Flt3*$^{ITD/ITD}$ mice lacking *Morrbid*, BM hypercellularity is completely rescued (Figures 1D and 1E). Taken together, these results suggest that *Morrbid* loss is able to partially correct the CMML and MPN phenotype in the setting of two distinct AML driver mutations, *Tet2* and *Flt3*^{ITD}.

Role of *MORRBID/Morrbid* in Human and Murine AML

We next aimed to extend these findings to assess the role of *Morrbid* in an aggressive form of AML driven by a combination of loss of *Tet2* and expression of *Flt3*$^{ITD/ITD}$ (i.e., *Tet2*$^{-/-}$; *Flt3*$^{ITD/ITD}$). We first mined the human AML gene expression database (unclassified, various subtypes included) as well as primary patient-derived AML samples to determine the contribution of *MORRBID* in human AML. As seen in Figure 2A, the presence of *MORRBID* is significantly higher in unclassified AML patients compared to normal control individuals. Furthermore, we also observed that a

Figure 1. *Morrbid*'s Role in *Tet2*-Mutation-Induced CMML and *Flt3*^{ITD}-Induced MPN

(A) Schematic for generating *Tet2*$^{-/-}$; *Morrbid*$^{-/-}$ (*TM*) and *Flt3*$^{ITD/ITD}$; *Morrbid*$^{-/-}$ (*FM*) compound mutant mice along with controls.

(B and C) Examination of peripheral blood (PB), bone marrow (BM), and spleen in the four experimental groups: wild type (WT), *Tet2*$^{-/-}$ (*T*), *Morrbid*$^{-/-}$ (*M*), and *TM* (age, 12 months).

(D and E) Examination of PB, BM, and spleen in the four experimental groups: WT, *Flt3*$^{ITD/ITD}$ (*F*), *Morrbid*$^{-/-}$ (*M*), and *FM* (age, 2 months).

(B and D) Plots of PB cell counts (upper panel) and representative profiles of flow cytometry of mature myeloid cells (Mac1^{+}) and B cells (CD19^{+}) from BM (lower panel).

(C and, E) quantification of BM cellullarity and spleen weight.

n = ~4–19. *p < 0.05; **p < 0.01; ***p < 0.001; ****p < 0.0001.

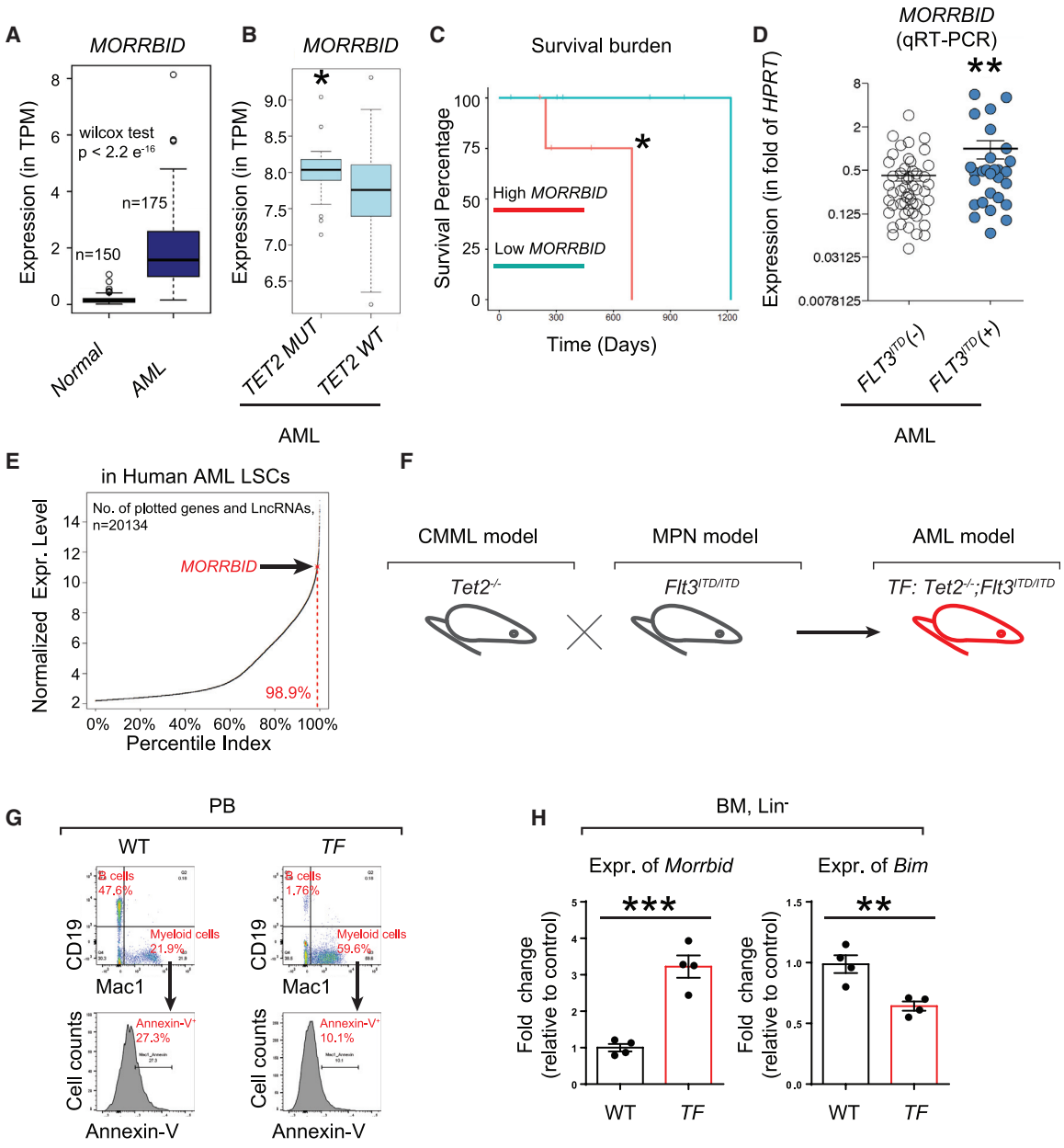

Figure 2. Highly Conserved Mammalian lncRNA *MORRBID*/*Morrbid* Is Hyperactivated in Human and Murine Models of AML

(A) Boxplot showing the expression levels of the *MORRBID* transcript in 150 normal whole-blood samples from the Genotype-Tissue Expression (GTEx) project compared against its expression in 175 AML samples from TCGA project. *p < $2.2e^{-16}$, Wilcoxon test.

(B) Boxplot showing the expression levels of *MORRBID* in BM samples of AML patients with *TET2* mutation (left) or WT *TET2* (right) from TCGA gene expression data. y axis represents the log-normalized gene expression level. p = 0.048, Mann-Whitney test.

(C) Overall survival of *TET2* mutated patients with high/low expression of *MORRBID*. A significant integrative effect of high expression *MORRBID* and *TET2* mutation in determining patient's overall survival was observed compared to low expression of *MORRBID*. *p = 0.047.

(D) Increased expression of *MORRBID* in AML cells with $FLT3^{ITD}$ mutation ($FLT3^{ITD(+)}$) compared to AML cells without $FLT3^{ITD}$ mutation ($FLT3^{ITD(-)}$). Mononuclear cells derived from AML patients negative for $FLT3^{ITD}$ (left) or positive for $FLT3^{ITD}$ (right) were subjected to qRT-PCR for *MORRBID* expression. n = 29 $FLT3^{ITD(+)}$ AML and 63 $FLT3^{ITD(-)}$ AML. **p < 0.01, Student's t test.

(E) Scatterplot of normalized gene expression level showing the top 1.1% percentile of *MORRBID* expression level among 20,134 genes and lncRNAs in nine bulk human AML stem cell samples.

(F) Murine model of AML used in the present study. $Flt3^{ITD/ITD}$ mice (*F*) were bred with $Tet2^{-/-}$ mice (*T*) to generate $Tet2^{-/-}$; $Flt3^{ITD/ITD}$ mice (*TF*).

(G) Representative apoptosis profiles in myeloid cells ($Mac1^{+}$) of WT and *TF* mice determined by Annexin-V staining (n = 4).

(H) Expression of *Morrbid* and *Bim* in Lin^{-} cells analyzed by qRT-PCR. **p < 0.01; ***p < 0.001.

CellPress
OPEN ACCESS

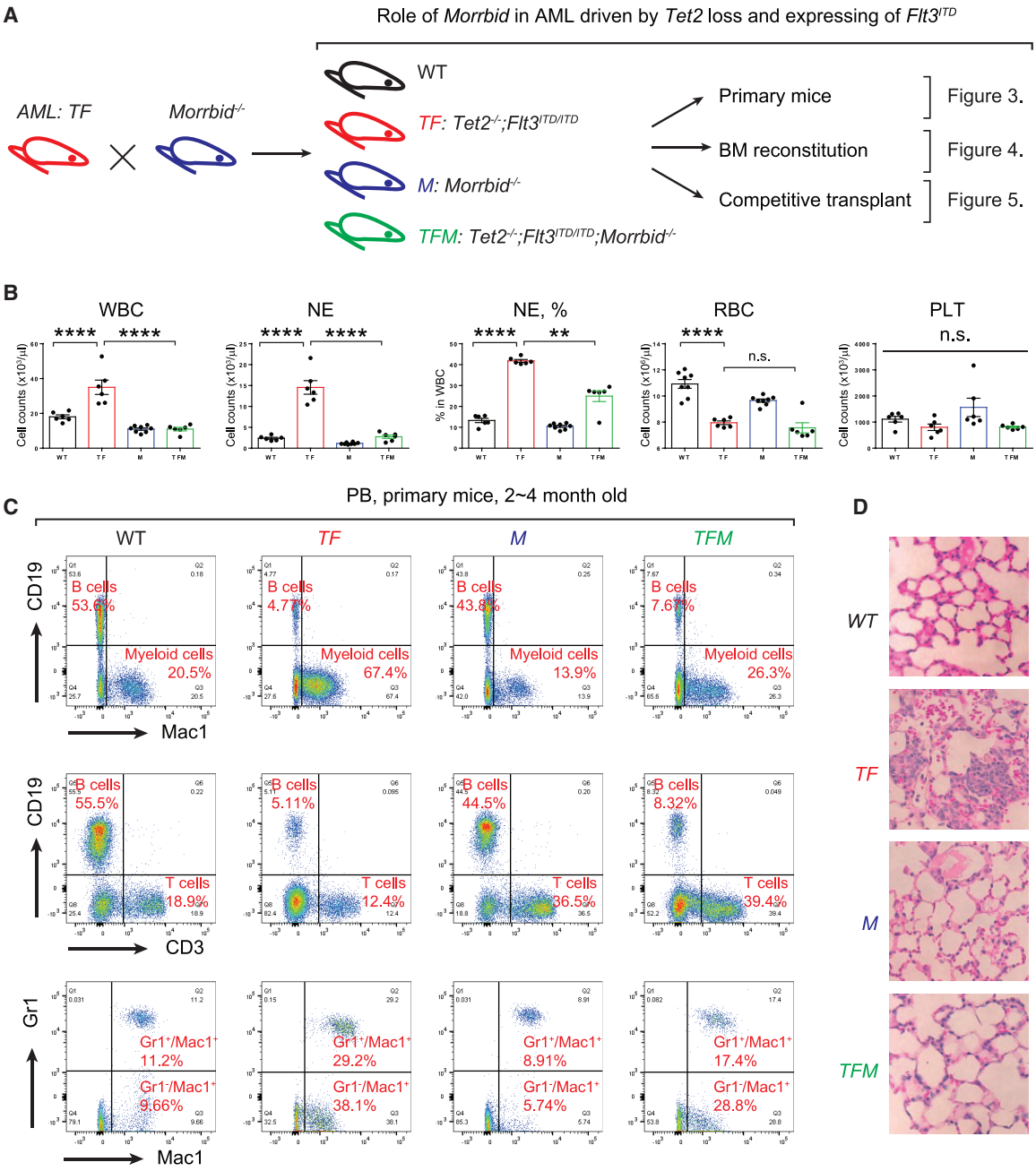

Figure 3. Genetic Loss of *Morrbid* in the Context of *Tet2*$^{-/-}$;*Flt3*$^{ITD/ITD}$ Mice Rescues Myeloid Cell Abnormalities

(A) A schematic describing various experimental approaches utilized to study the role of *Morrbid* in driving AML. *TF* mice were bred with *Morrbid*$^{-/-}$ mice to generate *Tet2*$^{-/-}$; *Flt3*$^{ITD/ITD}$; *Morrbid*$^{-/-}$ mice, indicated as *TFM*. The impact of *Morrbid* deficiency was analyzed in the original *TF* mice (primary mice) by utilizing BM cells derived from these mice and transplanting them into WT recipients and conducting competitive transplant experiments utilizing donors from *TF* and *TFM* mice along with normal WT competitors.

(B) Examination of PB parameters in the four experimental groups: WT, *TF*, *TFM*, and *M*. Shown are WBC, NE, RBC, and PLT counts as well as the frequency of NEs in various experimental groups. NE, neutrophil. PLT, platelet. RBC, red blood cell. WBC, white blood cell.

(C) Representative flow cytometry plots from PB of the four genotypes. Cells were stained with a combination of antibodies recognizing CD19 (B cells), Mac1 (myeloid cells), CD3 (T cells), and Gr1 (myeloid cells) markers. The percentage of various subsets are indicated in each quadrant in red.

(D) Lung histology from the four experimental groups. Infiltration of leukemic cells in the lung of *TFM* mice was reduced compared to *TF* mice.

n = 4–10; **p < 0.01; ****p < 0.0001.

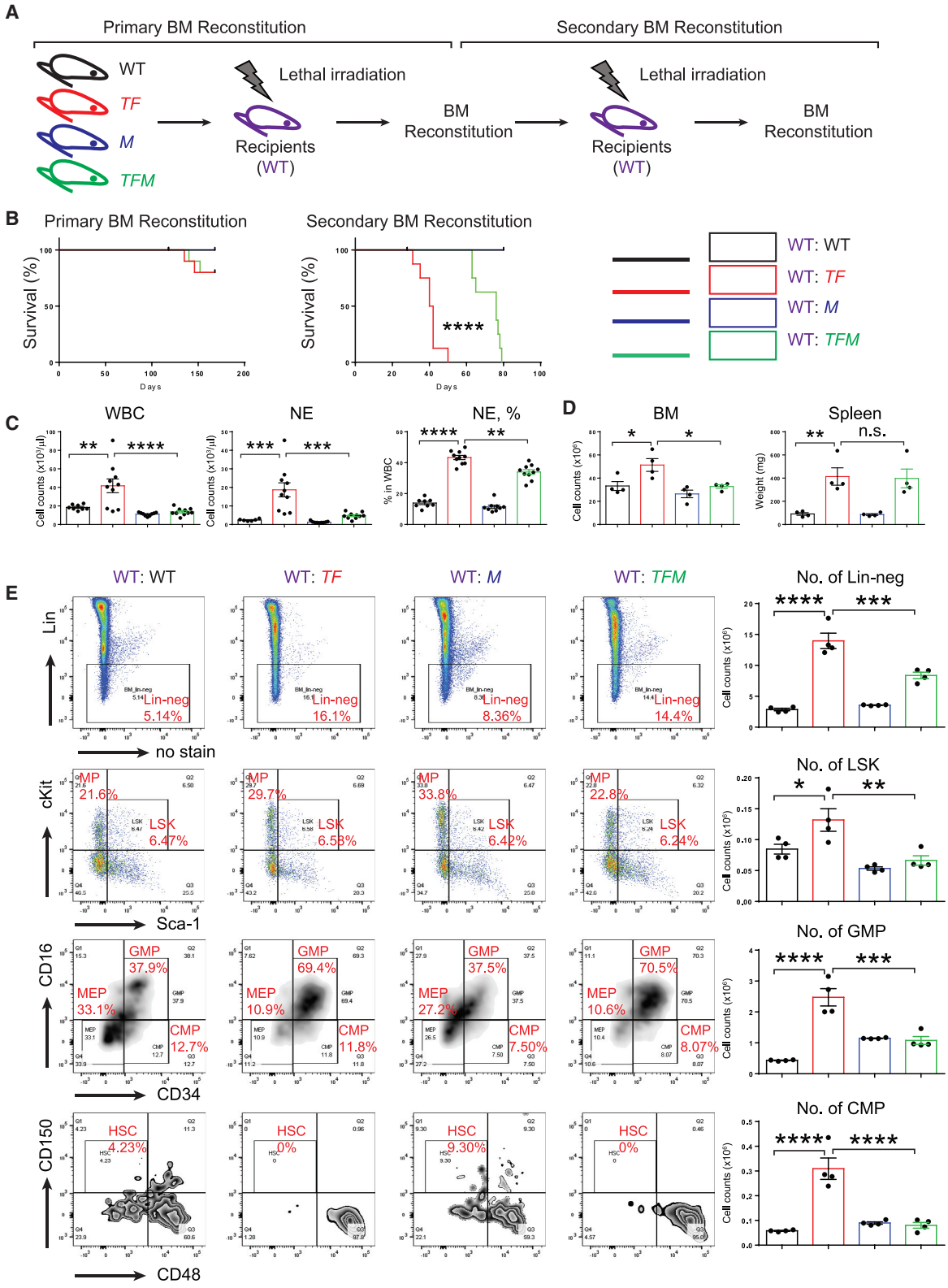

(legend on next page)

subset of AML patients bearing *TET2* mutations show significantly higher expression of *MORRBID* ($p = 0.048$ by Mann-Whitney test) and worse overall survival compared to AML patients lacking *TET2* mutations ($p = 0.047$ by log-rank test) from The Cancer Genome Atlas (TCGA) data (Figures 2B and 2C). Likewise, in AML samples collected from our own institution, AML patients with $FLT3^{ITD}$ mutations manifest ~3-fold higher expression of *MORRBID* compared to AML patients without $FLT3^{ITD}$ mutations (Figure 2D). Analysis on another independent dataset with expression of 20,134 genes, including lncRNAs, further confirmed that *MORRBID* is expressed in human leukemic stem cell (LSC) samples and its expression level is among top 1.1% percentile (Figure 2E). Taken together, these results suggest that hyperactivation of *MORRBID* is highly associated with *TET2* and $FLT3^{ITD}$ mutations in human AML (Figures 2B–2D) or even unclassified AML (Figures 2A and 2E).

To evaluate the potential functional significance of *MORRBID* in AML, we next utilized a murine model of AML induced by the loss of *Tet2* and expression of $Flt3^{ITD}$ ($Tet2^{-/-}$;$Flt3^{ITD/ITD}$, *TF*) (Figure 2F). Consistent with a previous report (Shih et al., 2015), *TF* mice manifest full penetration of abnormalities and high percentage of myeloid cells in the circulation (percentage of $Mac1^+$; 21.9% in WT versus 59.6% in *TF*), while B cell development is repressed (percentage of $CD19^+$: 47.6% in WT versus 1.76% in *TF*). Additionally, flow cytometry analysis with apoptosis marker Annexin-V showed that $Mac1^+$ cells in *TF* mice are resistant to cell death (percentage of Annexin-V^+: 27.3% in WT versus 10.1% in *TF*) (Figure 2G). Importantly, expression of *Morrbid* is significantly greater in BM Lin^- cells derived from *TF* mice compared to WT mice, and expression of the gene encoding pro-apoptotic protein Bim (also known as *Bcl2l11*) is significantly reduced in *TF* Lin^- cells (Figure 2H). Given these findings, we hypothesized that *TF* model of AML is suitable to study the functional consequences of Bim induction in the absence of *Morrbid*. We therefore generated mutants of *TF* lacking *Morrbid* ($Tet2^{-/-}$;$Flt3^{ITD/ITD}$;$Morrbid^{-/-}$;*TFM*) and all the necessary controls (Figure 3A). We conducted three different experiments to define the functional requirement of *Morrbid* in induction and prevention of AML driven by *TF* in (1) primary *TF* and *TFM* mice, (2) BM-derived recipient animals with *TF* or *TFM* donors, and (3) BM-reconstituted recipients with competitor donors (BoyJ WT donor's versus *TF* or *TFM* donors) (Figures 3A, 4A, and 5A). In all three scenarios, *TFM* mice or recipient mice with *TFM* donors manifest reduced WBC, NE and MO counts compared to controls (Figures 3B and 4C). Similar to our findings described earlier in *TM* and *FM* mutant mice (Figures 1 and 2), loss of *Morrbid* was unable to rescue the defects associated with RBCs in *TFM* mice (Figure 3B). In contrast, loss of *Morrbid* in *TF*-driven AML, reduced the leukemic cell percentage in PB and mitigated their infiltration into the lung of *TFM* mice (Figures 3C and 3D). Importantly, loss of *Morrbid* in the setting of *TF* cells extended the survival of BM-reconstituted animals with *TF* donors relative to controls in secondary transplant recipients (Figure 4B). Furthermore, while not changing the differentiation abnormalities in Lin^--$Sca1^+$-$cKit^+$ cells (LSKs), common myeloid progenitors (CMPs), and granulocyte-monocyte progenitors (GMPs), loss of *Morrbid* reduced the BM cellularity and absolute number of progenitor cells, including Lin^-,LSK, GMP, and CMP cells, in the BM of recipient mice transplanted with *TFM* donor cells compared to controls (Figures 4D and 4E). In experiments involving competitive transplantation, loss of *Morrbid* in the setting of *TF* also mitigated the clonal expansion observed using *TF* cells in PB and BM (Figures 5B, 5C, and 5E). Loss of *Morrbid* in the setting of *TF* was also slightly but significantly able to increase the portion of B cells (Figure 5G). Additionally, the increase in spleen size associated with *TF* donors was completely rescued when cells were transplanted using *TFM* donors under a competitive setting using BoyJ cells as competitors (Figure 5F), further supporting the notion that loss of *Morrbid* represents a novel therapeutic strategy for AML treatment.

Given the significant correction of phenotype observed in *TFM* mice, we next sought to determine the extent to which loss of *Morrbid* impacts apoptosis in various compartments of the BM, including $Mac1^+$ cells, myeloid progenitor (MP) cells (Lin^--$cKit^+$-$Sca1^-$), and LSK cells. As seen in Figure 6A, the reduction in apoptosis observed in $Mac1^+$, MP, and LSK cells associated with *TF* mice was partially reversed in the *TFM* mice. Consistently, an increase in the expression of Bim in *TFM* cells was determined by both qRT-PCR and mean fluorescence intensity (MFI) assays (Figures 6B and 6C). Taken together, these results suggest that targeting *Morrbid* induces apoptosis in leukemic cells. Although the mechanism of transcriptional repression of Bim by *Morrbid* via DNA loop in *cis* was initially addressed in our previous studies (Kotzin et al., 2016), future studies are required to assess the extent to which *Morrbid* itself, rather than the act of its transcription, may be the primary mediator of *Bim* regulation.

To evaluate if there is any substantial functional difference between BCL-2/MCL-1 inhibition and *Morrbid* targeting, we treated *TF* mice with single-agent ABT-199 (a selective inhibitor of BCL-2), S63845 (a selective inhibitor of MCL-1), or 5-azacytidine (an effective drug for *TET2*-mutation-related myelodysplastic syndromes [MDS]) or with various combinations (Figure 7A; DiNardo et al., 2019; Pollyea et al., 2018). Although a high dose of ABT-199 and 5-azacytidine is toxic to the animal (data not shown), *TF* mice are resistant to treatment with any of the single agents at low dose or with a combination treatment of low dose ABT-199 and S63845 (Figures 7A and 7B). A drug regimen with a low dose of all three drugs (ABT-199 + S63845 + 5-azacytidine) is sufficient to reduce WBCs, NEs, and MOs in *TF* mice after

Figure 4. Increased Survival of Mice Transplanted with *TFM* Donor Cells Compared to *TF* Cells

(A) A schematic of recipient mice undergoing primary and secondary transplantation using BM derived donor cells from the four genotypes.

(B) Enhanced survival of recipient mice transplanted with *TFM* donor cells in secondary recipients compared to *TF* donors.

(C and D) Loss of *Morrbid* in the setting of *TF* cells rescues WBC and NE counts as well as NE frequency and BM cellularity, but not spleen size. (C) Samples from PB. D, samples from BM and spleen.

(E) *Morrbid* deficiency in the context of *TF* cells rescues the absolute number of Lin^- cells, LSK cells, granulocyte-macrophage progenitors (GMPs), and common myeloid progenitors (CMPs) to near-WT levels.

n = 4–10; *$p < 0.05$; **$p < 0.01$; ***$p < 0.001$; ****$p < 0.0001$.

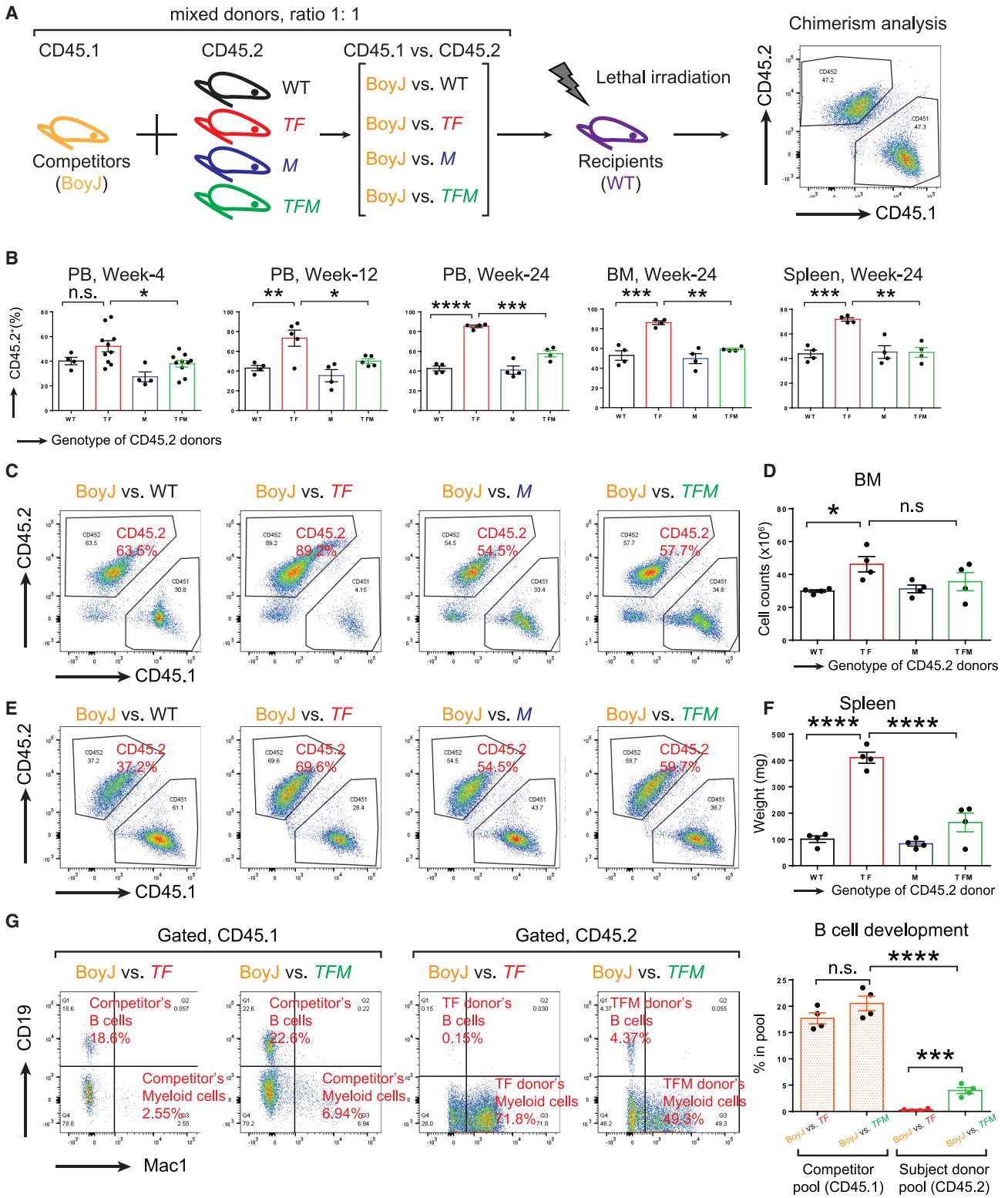

Figure 5. Growth Advantage of *TF* Cells Was Mitigated When *Morrbid* Is Depleted

(A) Donor cells from *TF* or *TFM* mice along with WT and *Morrbid*$^{-/-}$ controls were mixed with BoyJ cells in identical cell number (0.5×10^6 versus 0.5×10^6) for a competitive transplantation assay.

(B) Chimerism analysis of PB, BM, and spleen samples from chimeric mice at the indicated time points post transplantation.

(legend continued on next page)

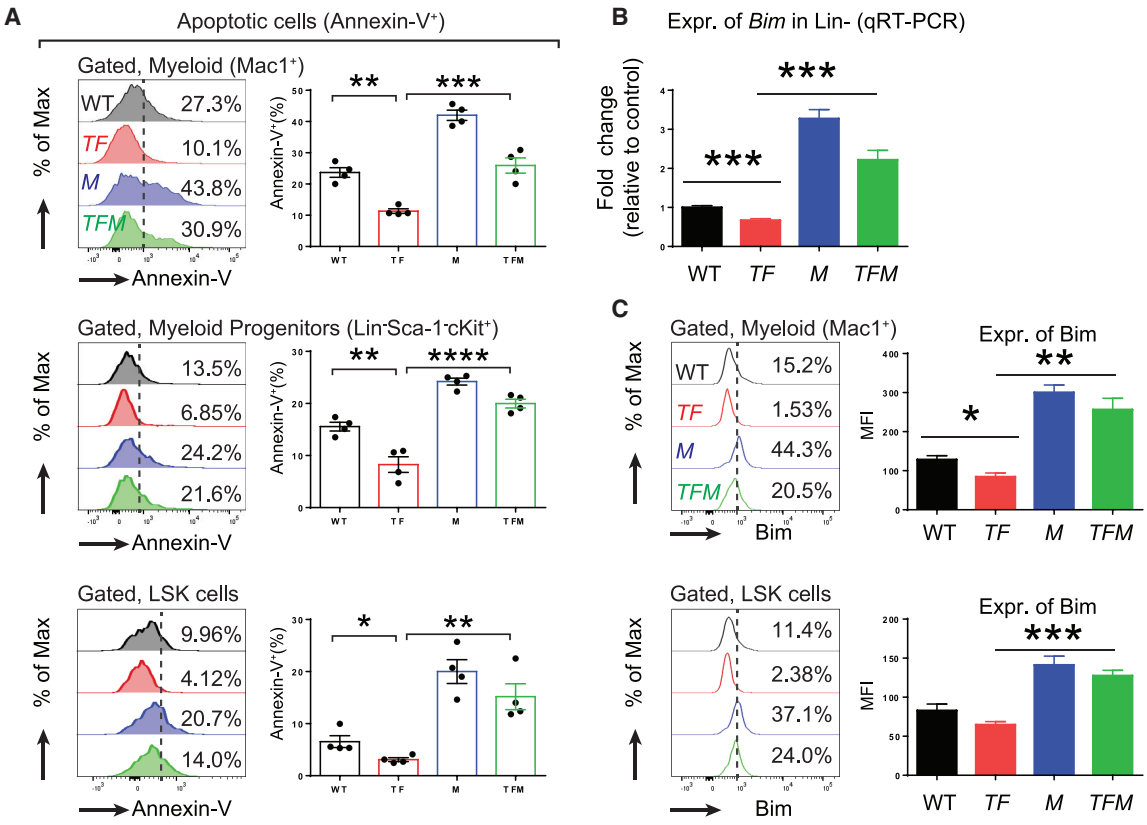

Figure 6. *Morrbid* Loss Induces Increased Expression of Bim and Apoptosis in Leukemic Cells, Including Mature Myeloid Cells (Mac1$^+$), Myeloid Progenitor Cells (Lin$^-$Sca-1$^-$cKit$^+$), and LSK Cells

(A) Level of apoptosis as determined by Annexin-V staining.

(B) Expression of *Bim* in Lin$^-$ cells as analyzed by qRT-PCR.

(C) Expression of Bim in myeloid cells and LSK cells as analyzed by intracellular staining of Bim and quantified by mean fluorescence intensity (MFI).

n = 4; *p < 0.05; **p < 0.01; ***p < 0.001; ****p < 0.0001.

three cycles of treatment (Figure 7B). However, this treatment failed to improve RBC counts (Figure 7B). Although the ratio of mature myeloid cells and B cells was slightly altered in the PB, BM, and spleen (Figure 7C), analysis of hematopoiesis on hematopoietic progenitors such as LSKs, CMPs and GMPs in the drug treated *TF* mice showed that this treatment failed to change the differentiation abnormalities associated with *TF* mice in the BM and spleen (data not shown). Future experiments are required to compare the impact of Bcl-2 repression via ABT-199 in *TFM* mice and *TF* mice to assess whether direct repression of Bcl-2 in *TFM* mice further improves the AML phenotype.

In summary, we have defined a critical role for a novel myeloid regulator *Morrbid* in a spectrum of myeloid neoplasms, including CMML, MPN, and AML. Our results show that *Morrbid* is a myeloid-specific cell survival regulator not only in physiologic conditions but also in leukemic conditions.

STAR★METHODS

Detailed methods are provided in the online version of this paper and include the following:

- KEY RESOURCES TABLE
- RESOURCE AVAILABILITY
  - Lead Contact
  - Materials Availability
  - Data and Code Availability
- EXPERIMENTAL MODEL AND SUBJECT DETAILS
  - MICE
  - Human Blood Samples
- METHOD DETAILS
  - Mouse Experimental Procedures
  - qRT-PCR analysis of *MORRBID* using human AML blood samples

(C and E) Representative chimerism profiles in BM (C) and spleen samples (E).

(D and F) BM cellularity (D) and spleen weight (F) were examined at 6 months post-transplantation.

(G) In chimeric mice, the portion of B cells is partially corrected in recipient mice transplanted with *TFM* donors.

Student's t test (n = 4–10); *p < 0.05; **p < 0.01; ***p < 0.001; ****p < 0.0001.

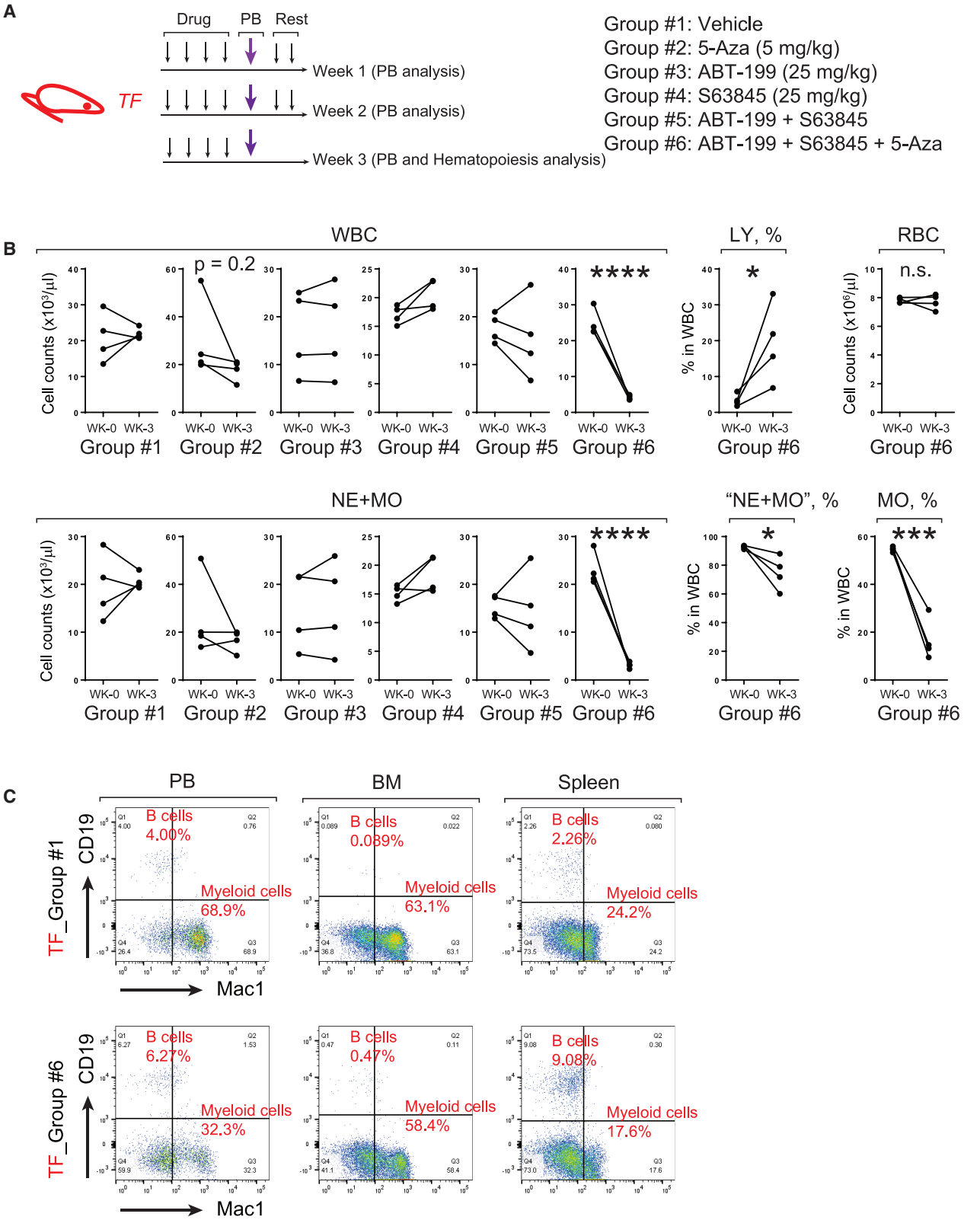

(legend on next page)

ACKNOWLEDGMENTS

We thank our colleagues for technical support, critically reading our manuscript, and their suggestions to improve the manuscript. We would also like to thank Ms. Tracy Winkle for her administrative support. This work was supported in part by grants from the National Institutes of Health (R01-CA134777, R01-HL140961, R01-HL146137, and R01-CA173852 to R.K.) and by funds to R.K. from the Riley Children's Foundation. Z.C. is supported by National Institutes of Health grant T32HL007910.

AUTHOR CONTRIBUTIONS

Z.C. and R.K. conceived and designed the experiments, analyzed data, and wrote the manuscript. Z.C. performed most of the experiments and acquired the data. F.A. and B.R. assisted with certain experiments and acquired part of the data. S.V.D., S.C.J., and C.Z. did the bioinformatics analysis. J.J.K., M.C., G.W., A.W., and J.H.-M. contributed reagents and did the qRT-PCR for *MORRBID* and genotyping of $FLT3^{ITD}$ in human AML patients.

DECLARATION OF INTERESTS

The authors declare no competing interests.

Received: February 27, 2020
Revised: April 30, 2020
Accepted: June 3, 2020
Published: June 23, 2020

REFERENCES

Anstee, N.S., Bilardi, R.A., Ng, A.P., Xu, Z., Robati, M., Vandenberg, C.J., and Cory, S. (2019). Impact of elevated anti-apoptotic MCL-1 and BCL-2 on the development and treatment of MLL-AF9 AML in mice. Cell Death Differ. *26*, 1316–1331.

Ashkenazi, A., Fairbrother, W.J., Leverson, J.D., and Souers, A.J. (2017). From basic apoptosis discoveries to advanced selective BCL-2 family inhibitors. Nat. Rev. Drug Discov. *16*, 273–284.

Caenepeel, S., Brown, S.P., Belmontes, B., Moody, G., Keegan, K.S., Chui, D., Whittington, D.A., Huang, X., Poppe, L., Cheng, A.C., et al. (2018). AMG 176, a selective MCL1 inhibitor, is effective in hematologic cancer models alone and in combination with established therapies. Cancer Discov. *8*, 1582–1597.

Cai, Z., Kotzin, J.J., Ramdas, B., Chen, S., Nelanuthala, S., Palam, L.R., Pandey, R., Mali, R.S., Liu, Y., Kelley, M.R., et al. (2018). Inhibition of inflammatory signaling in Tet2 mutant preleukemic cells mitigates stress-induced abnormalities and clonal hematopoiesis. Cell Stem Cell *23*, 833–849.e5.

Chu, S.H., Heiser, D., Li, L., Kaplan, I., Collector, M., Huso, D., Sharkis, S.J., Civin, C., and Small, D. (2012). FLT3-ITD knockin impairs hematopoietic stem cell quiescence/homeostasis, leading to myeloproliferative neoplasm. Cell Stem Cell *11*, 346–358.

DiNardo, C.D., Pratz, K., Pullarkat, V., Jonas, B.A., Arellano, M., Becker, P.S., Frankfurt, O., Konopleva, M., Wei, A.H., Kantarjian, H.M., et al. (2019). Venetoclax combined with decitabine or azacitidine in treatment-naive, elderly patients with acute myeloid leukemia. Blood *133*, 7–17.

Hanahan, D., and Weinberg, R.A. (2011). Hallmarks of cancer: the next generation. Cell *144*, 646–674.

Huang, K., O'Neill, K.L., Li, J., Zhou, W., Han, N., Pang, X., Wu, W., Struble, L., Borgstahl, G., Liu, Z., et al. (2019). BH3-only proteins target BCL-xL/MCL-1, not BAX/BAK, to initiate apoptosis. Cell Res. *29*, 942–952.

Jaiswal, S., and Ebert, B. (2019). Clonal hematopoiesis in human aging and disease. Science *366* (*6465*), eaan4673.

Kikushige, Y., Yoshimoto, G., Miyamoto, T., Iino, T., Mori, Y., Iwasaki, H., Niiro, H., Takenaka, K., Nagafuji, K., Harada, M., et al. (2008). Human Flt3 is expressed at the hematopoietic stem cell and the granulocyte/macrophage progenitor stages to maintain cell survival. J. Immunol. *180*, 7358–7367.

Kotzin, J.J., Spencer, S.P., McCright, S.J., Kumar, D.B.U., Collet, M.A., Mowel, W.K., Elliott, E.N., Uyar, A., Makiya, M.A., Dunagin, M.C., et al. (2016). The long non-coding RNA Morrbid regulates Bim and short-lived myeloid cell lifespan. Nature *537*, 239–243.

Lee, B.H., Tothova, Z., Levine, R.L., Anderson, K., Buza-Vidas, N., Cullen, D.E., McDowell, E.P., Adelsperger, J., Fröhling, S., Huntly, B.J., et al. (2007). FLT3 mutations confer enhanced proliferation and survival properties to multipotent progenitors in a murine model of chronic myelomonocytic leukemia. Cancer Cell *12*, 367–380.

Li, Z., Cai, X., Cai, C.-L., Wang, J., Zhang, W., Petersen, B.E., Yang, F.-C., and Xu, M. (2011). Deletion of Tet2 in mice leads to dysregulated hematopoietic stem cells and subsequent development of myeloid malignancies. Blood *118*, 4509–4518.

Majeti, R., Becker, M.W., Tian, Q., Lee, T.-L.M., Yan, X., Liu, R., Chiang, J.-H., Hood, L., Clarke, M.F., and Weissman, I.L. (2009). Dysregulated gene expression networks in human acute myelogenous leukemia stem cells. Proc. Natl. Acad. Sci. USA *106*, 3396–3401.

McBride, A., Houtmann, S., Wilde, L., Vigil, C., Eischen, C.M., Kasner, M., and Palmisiano, N. (2019). The role of inhibition of apoptosis in acute leukemias and myelodysplastic syndrome. Front. Oncol. *9*, 192.

Mead, A.J., Kharazi, S., Atkinson, D., Macaulay, I., Pecquet, C., Loughran, S., Lutteropp, M., Woll, P., Chowdhury, O., Luc, S., et al. (2013). FLT3-ITDs instruct a myeloid differentiation and transformation bias in lymphomyeloid multipotent progenitors. Cell Rep. *3*, 1766–1776.

Mead, A.J., Neo, W.H., Barkas, N., Matsuoka, S., Giustacchini, A., Facchini, R., Thongjuea, S., Jamieson, L., Booth, C.A.G., Fordham, N., et al. (2017). Niche-mediated depletion of the normal hematopoietic stem cell reservoir by Flt3-ITD-induced myeloproliferation. J. Exp. Med. *214*, 2005–2021.

Merino, D., Kelly, G.L., Lessene, G., Wei, A.H., Roberts, A.W., and Strasser, A. (2018). BH3-mimetic drugs: blazing the trail for new cancer medicines. Cancer Cell *34*, 879–891.

Moran-Crusio, K., Reavie, L., Shih, A., Abdel-Wahab, O., Ndiaye-Lobry, D., Lobry, C., Figueroa, M.E., Vasanthakumar, A., Patel, J., Zhao, X., et al. (2011). Tet2 loss leads to increased hematopoietic stem cell self-renewal and myeloid transformation. Cancer Cell *20*, 11–24.

Naganna, N., Opoku-Temeng, C., Choi, E.Y., Larocque, E., Chang, E.T., Carter-Cooper, B.A., Wang, M., Torregrosa-Allen, S.E., Elzey, B.D., Lapidus, R.G., and Sintim, H.O. (2019). Amino alkynylisoquinoline and alkynylnaphthyridine compounds potently inhibit acute myeloid leukemia proliferation in mice. EBioMedicine *40*, 231–239.

Pollyea, D.A., Stevens, B.M., Jones, C.L., Winters, A., Pei, S., Minhajuddin, M., D'Alessandro, A., Culp-Hill, R., Riemondy, K.A., Gillen, A.E., et al. (2018). Venetoclax with azacitidine disrupts energy metabolism and targets leukemia stem cells in patients with acute myeloid leukemia. Nat. Med. *24*, 1859–1866.

Ramsey, H.E., Fischer, M.A., Lee, T., Gorska, A.E., Arrate, M.P., Fuller, L., Boyd, K.L., Strickland, S.A., Sensintaffar, J., Hogdal, L.J., et al. (2018). A novel MCL1 inhibitor combined with venetoclax rescues venetoclax-resistant acute myelogenous leukemia. Cancer Discov. *8*, 1566–1581.

Figure 7. Treatment of *TF* AML Mice with BCL-2/MCL-1 Inhibitors and 5-Azacytidine

(A) Scheme for six different drug regimens.

(B) Alteration of PB parameters for each individual mouse from six different cohort.

(C) Representative profiles of myeloid cells and B cells in PB, BM, and spleen after treatments.

n = 4; *p < 0.05; ***p < 0.001; ****p < 0.0001.

Shih, A.H., Jiang, Y., Meydan, C., Shank, K., Pandey, S., Barreyro, L., Antony-Debre, I., Viale, A., Socci, N., Sun, Y., et al. (2015). Mutational cooperativity linked to combinatorial epigenetic gain of function in acute myeloid leukemia. Cancer Cell *27*, 502–515.

Shukla, S., Saxena, S., Singh, B.K., and Kakkar, P. (2017). BH3-only protein BIM: an emerging target in chemotherapy. Eur. J. Cell Biol. *96*, 728–738.

Teh, T.C., Nguyen, N.Y., Moujalled, D.M., Segal, D., Pomilio, G., Rijal, S., Jabbour, A., Cummins, K., Lackovic, K., Blombery, P., et al. (2018). Enhancing venetoclax activity in acute myeloid leukemia by co-targeting MCL1. Leukemia *32*, 303–312.

Yang, S., Mao, Y., Zhang, H., Xu, Y., An, J., and Huang, Z. (2019). The chemical biology of apoptosis: Revisited after 17 years. Eur. J. Med. Chem. *177*, 63–75.

STAR★METHODS

KEY RESOURCES TABLE

REAGENT or RESOURCE	SOURCE	IDENTIFIER
Experimental Models: Organisms/Strains		
Mouse: Tet2$^{-/-}$	Li et al., 2011	N/A
Mouse: Ft3$^{ITD/+}$	Lee et al., 2007	N/A
Mouse: Morrbid$^{-/-}$	Kotzin et al., 2016	N/A
Mouse: C57/B6	Jackson Laboratory	Cat #000664
Mouse: BoyJ	Jackson Laboratory	Cat #002014
Critical Commercial Assays		
EasySep Mouse Hematopoietic Progenitor Cell Isolation Kit	StemCell	#19856
Rneasy Mini Kit	QIAGEN	#74104
SuperScript II Reverse Transcriptase	Fisher Scientific	#18064014
SYBR Green master mix	Life Technologies	#4385612
Antibodies for Flow Cytometry		
TER-119, PE	BioLegend	#116208
Gr1, PE	BioLegend	#108408
Mac1, PE	BioLegend	#101208
B220, PE	BioLegend	#103208
CD3, PE	BioLegend	#100206
CD4, PE	BioLegend	#116006
CD8a, PE	BioLegend	#100708
c-Kit, APC	BioLegend	#105812
Sca-1, APC/Cy7	BioLegend	#108126
CD150, PE/Cy5	BioLegend	#115912
CD48, PE/Cy7	BioLegend	#103424
CD127, PE/Cy5	BioLegend	#135016
CD16/32, PE/Cy7	bioLegend	#101318
CD34, FITC	eBioscience	#11-0341-85
Annexin V, FITC	BioLegend	#640906
7-AAD	BioLegend	#79993
Bim mAb (C34C5), PE	Cell Signaling Tech	#12816S
Bim mAb (C34C5), AF488	Cell Signaling Tech	#94805S
CD45.2, PerCP/Cy5.5	BioLegend	#109928
CD45.1, PE/Cy7	BioLegend	#110730
CD19, APC	BioLegend	#115512
CD71, APC	eBioscience	#17-0711-82
Oligonucleotides		
Mouse_Actin-b, Forward: GACGGCCAGGTCATCACTATTG	Cai et al., 2018	N/A
Mouse_Actin-b, Reverse: AGGAAGGCTGGAAAAGAGCC	Cai et al., 2018	N/A
Mouse_Morrbid, Forward: TCTGAGAATGAGGGGACTGG	Kotzin et al., 2016	N/A
Mouse_Morrbid, Reverse: TGTGCTGTGAAGATCCCAAG	Kotzin et al., 2016	N/A
Human_HPRT, Forward: GCTATAAATTCTTTGCTGACCTGCTG	Kotzin et al., 2016	N/A

(*Continued on next page*)

Continued

REAGENT or RESOURCE	SOURCE	IDENTIFIER
Human_HPRT, Reverse: AATTACTTTTATGTCCCCTGTTGACTGG	Kotzin et al., 2016	N/A
Human_MORRBID, Forward: ACTGGATGGTCGCTGCTTTT	Kotzin et al., 2016	N/A
Human_MORRBID, Reverse: CTTCCCAGGAACTGTGCTGT	Kotzin et al., 2016	N/A
Software and Algorithms		
FlowJo	FlowJo	V10.2
Prism	GraphPad Software	V6.0
Adobe Illustrator	Adobe	CC-2015

RESOURCE AVAILABILITY

Lead Contact

Further information and requests for resources and reagents should be directed to and will be fulfilled by the Lead Contact, Reuben Kapur (rkapur@iupui.edu).

Materials Availability

All unique/stable reagents generated in this study are available from the Lead Contact with a completed Materials Transfer Agreement.

Data and Code Availability

This study did not generate any unique datasets or code.

EXPERIMENTAL MODEL AND SUBJECT DETAILS

MICE

All the animal experiments were approved and maintained by Laboratory Animal Resource Center at Indiana University School of Medicine. C57/B6 mice ($CD45.2^+$) were procured from IUSM core facility and used as wild-type controls. For transplantation studies, congenic BoyJ mice ($CD45.1^+$) or F1 mice ($CD45.1^+CD45.2^+$) were procured from IUSM core facility and used as wild-type controls. CMML model mice (*Tet2*$^{-/-}$), MPN model mice (*Flt3*$^{ITD/+}$) and *Morrbid* deficient mice (*Morrbid*$^{-/-}$) have been described (Kotzin et al., 2016; Lee et al., 2007; Li et al., 2011) and were bred for generating the compound mutants. Age matched mice (both male and female) were analyzed: for CMML analysis, mouse sample were collected at old age (~12 month old); for MPN analysis, mouse sample were collected at young age (~2 month old); for AML analysis, mouse sample were collected at large-range of age as indicated (2~6 month old or 2~6 month post the transplantation).

Human Blood Samples

Peripheral blood (PB) samples of human AML patients (both male and female) enrolled in our affiliated hospital were obtained from our blood bank with approved protocol.

METHOD DETAILS

Mouse Experimental Procedures

Analysis procedures involving mouse experiments (i.e., flow cytometry strategies and Annexin-V gating and intracellular staining for anti-Bim) have been in described in detail in our recent study (Cai et al., 2018).

qRT-PCR analysis of *MORRBID* using human AML blood samples

Peripheral blood of AML patients enrolled in our affiliated hospitals were sorted for monocytes and then analyzed by qRT-PCR for determining the association between *MORRBID* expression and *FLT3*^{ITD} mutation. Expression of *HPRT* was used as internal control. Genomic DNA from blood samples was also purified and *FLT3*^{ITD} mutation was determined by PCR genotyping.

Bioinformatic analysis of MORRBID and survival burden in human AML

To identify which lncRNAs potentially associated with AML, we downloaded raw RNA-seq data for 175 AML samples from TCGA, along with the pertaining patient clinical data. The downloaded data was aligned to the human reference genome (GRCh38) using

HISAT2 and transcript abundance was computed using StringTie. Microarray data of the TCGA AML samples were also downloaded and analyzed. Genome scale survival analysis was performed over the AML expression and clinical data obtained from TCGA, using survival R package (https://github.com/therneau/survival), to obtain the survival statistics for all human lncRNAs obtained from Gencode v24. The top 20 (sorted ascending by FDR) lncRNAs including *MORRBID* were extracted for further analysis. Simultaneously, we downloaded 150 normal whole blood gene abundance data from the GTEx project to observe and compare lncRNA expression levels across AML and normal whole blood. Log-rank test was used to test the prognostic association of *MORRBID* in the AML patients with *TET2* mutations. 17 *TET2* mutated samples with both gene expression and mutation were analyzed. High and low expression level of *MORRBID* was determined by higher than 65% quantile and lower than 35% quantile of its expression level. To demonstrate the significant expression of *MORRBID* in human AML leukemic stem cells, we retrieved the dataset GSE17054 from NCBI GEO database (Majeti et al., 2009), which contains 9 samples of bulk leukemic stem cell (LSC) samples collected from AML patients. We compared the averaged expression of *MORRBID* versus other genes in the 9 AML LSC samples. Our analysis suggests *MORRBID* is among the top 1.1% expressed genes and lncRNA in all the measured probes.

QUANTIFICATION AND STATISTICAL ANALYSIS

All experimental procedures on mice were run in parallel with proper controls (sex and age matched littermate controls when possible) for observing experiment variabilities. Analysis of grouped data was not blinded and no samples were excluded. If not specified, P value was calculated using an unpaired t test for comparing means of two groups (GraphPad Prism 6.0). Error bars indicate the standard error of mean (s.e.m.).